Charles University
Second Faculty of Medicine

Summary of Dissertation

Glial cells in progression of Amyotrophic lateral sclerosis

Gliové buňky v progresi amyotrofické laterální sklerózy

Tereza Filipi

Prague, 2024

The Dissertation was written during a full-time doctoral study program in Neurosciences at the Department of Cellular Neurophysiology, The Institute of Experimental Medicine, CAS.

Supervisor: Ing. Miroslava Anděrová, CSc.,
Department of Cellular Neurophysiology, Institute of Experimental Medicine, CAS, Vídeňská 1083, 142 00, Prague 4

Opponents:

The defense will take place before the Board for the Defense of the Subject program of Neurosciences on..... in..... from ..... hours

The Chairman of the Subject Area Board and guarantor of the doctoral study Neurosciences program prof. MUDr. Jan Laczó, Ph.D.,
Department of Neurology, Second Faculty of Medicine, Charles University, University Hospital, V Úvalu 84, 150 06, Prague 5

The Dean of the Faculty: prof. MUDr. Marek Babjuk, CSc.

The work has been supported by grants of Czech Science Foundation: 23-05327S, 19-02046S and by the Charles University Grant Agency (Grant Number 158320).

The dissertation is available for inspection at the Department for Ph.D. Study of the Dean´s Office, Second Faculty of Medicine, Charles University, V Úvalu 84, 150 06 Praha 5 (phone 224 435 836).

Glial cells in progression of Amyotrophic lateral sclerosis

Abstract

Glial cells are known to support neurons, maintain homeostasis in the nervous system or act as an immune defense, to name a few of their physiological functions. In pathological conditions, they change their properties and become active participants with beneficial and/or harmful effects. The exact role they play in Amyotrophic lateral sclerosis (ALS) is not known, but with the urgent need for efficient therapy, there is a constant effort to precisely elucidate their involvement. We examined cortical astrocytes, microglia and oligodendrocytes in the SOD1(G93A) mouse model of ALS with the use of single-cell RNA sequencing and immunohistochemistry, and then further focused on the functional properties of astrocytes in ALS and in Alzheimer's disease (AD) using *in situ* 3D-morphometry and the real-time iontophoretic method. The profiling revealed minimal changes in the cortical glia in the final stage of ALS, suggesting unsuitability of the model for future cortical studies. Nevertheless, with the use of the ALS mouse model on a different background, we were able to detect cortical and spinal astrogliosis and identify diminished K^+ uptake during hyperkalemia and downregulation of Kir4.1 in spinal ALS-affected astrocytes. The investigation in the AD model also showed diminished astrocytic swelling in response to hyperkalemia and hypo-osmotic stress. The overall results provide insights into the astrocytic homeostatic abilities during pathology and highlight the importance of using a reliable animal model.

Keywords

AD, ALS, astrocytes, microglia, oligodendrocytes, potassium uptake

Gliové buňky v progresi amyotrofické laterální sklerózy

Abstrakt

Gliové buňky jsou známy tím, že poskytují podporu neuronům, zajišťují homeostázu v nervovém systému nebo se účastní imunitních reakcí, což je ale jen několik z jejich mnoha fyziologických funkcí. Během patologií se však jejich funkce a vlastnosti mění a glie jsou aktivními účastníky s potenciálně protektivním a/nebo škodlivým účinkem. Přesná role gliových buněk v progresi Amyotrofické laterální sklerózy (ALS) není dosud známa, ale vzhledem k nutnosti efektivní léčby se na jejím objasnění neustále pracuje. My jsme se věnovali kortikálním astrocytům, mikrogliím a oligodendrocytům v myším modelu SOD1(G93A) s využitím sekvenování na úrovni jedné buňky a imunohistochemie a poté jsme se detailněji zaměřili na funkční vlastnosti astrocytů v průběhu ALS a také Alzheimerovy choroby (AD) s pomocí *in situ* 3D-morfometrie a iontoforetické metody v reálném čase. Profilování odhalilo pouze mírné změny u kortikálních glií ve finálním stádiu nemoci, což naznačuje nevhodnost tohoto modelu pro další studie zaměřené na mozkovou kůru. S využitím myšího ALS modelu s odlišným genetickým pozadím jsme nicméně identifikovali astrogliózu v mozkové kůře i v míše, společně se sníženým vychytáváním K^+ iontů a sníženou expresí Kir4.1 u míšních astrocytů. Experimenty v AD modelu ukázaly rovněž snížené vychytávání K^+ iontů během hyperkalémie i hypoosmotického stresu. Celkově naše výsledky poskytly vhled do homeostatických schopností astrocytů během patologie a ukázaly důležitost využití spolehlivého animálního modelu pro výzkum.

Klíčová slova

AD, ALS, astrocyty, mikroglie, oligodendrocyty, vychytávání draslíku

Table of Contents

1 BACKGROUND 8

1.1 Amyotrophic lateral sclerosis 8

1.2 Glia in ALS 8

1.3 Alzheimer´s disease 10

2 OBJECTIVES 12

3 MATERIALS AND METHODOLOGY 14

3.1 Animals 14

3.2 Behavioral testing 14

3.3 Preparation of acute brain and spinal cord slices 14

3.4 Three-dimensional confocal morphometry 15

3.5 Real time iontophoretic method 15

3.6 Preparation of single-cell suspension 15

3.7 Single cell RNA-Sequencing 16

3.8 RNA-Sequencing data analysis 16

3.9 Immunohistochemistry and confocal microscopy 16

3.10 Cerebrospinal fluid (CSF) isolation and elemental analysis 17

3.11 Statistics 17

4 RESULTS 18

4.1 Characterization of the SOD1(G93A) mouse model phenotype and pathological traits in the motor cortex 18

4.2 Functional properties of astrocytes in a mouse model of ALS 22

4.3 Astrocyte swelling during hyperkalemia in the model of AD 27

5 DISCUSSION 28

5.1 Characterization of SOD1(G93A) the Mouse Model Phenotype and Pathological Traits in the Motor Cortex 28

5.2 Functional Properties of Astrocytes in a Mouse Model of ALS 29

5.3 Functional Properties of Astrocytes in the Model of Alzheimer´s Disease 31

6 CONCLUSIONS 32

7 SUMMARY IN ENGLISH 34

7.1 Characterization of SOD1(G93A) Mouse Model Phenotype and Pathological Traits in the Motor Cortex 34

7.2 Functional Properties of Astrocytes in a Mouse Model of Amyotrophic lateral sclerosis 34

7.3 Functional Properties of Astrocytes in the Model of Alzheimer´s Disease 34

8 SUMMARY IN CZECH 36

8.1 Charakterizace fenotypu a patologie v mozkové kůře myšího modelu SOD1(G93A) 36

8.2 Funkční vlastnosti astrocytů v myším modelu Amyotrofické laterální sklerózy 36

8.3 Funkční vlastnosti astrocytů v myším modelu Alzheimerovy choroby36

9 REFERENCES 38

10 LIST OF PUBLICATIONS 46

1 BACKGROUND

1.1 Amyotrophic lateral sclerosis

Amyotrophic lateral sclerosis (ALS) is a fatal disease during which the motor neurons (MNs) in the motor cortex, brainstem and spinal cord degenerate. The disease is progressive and culminates in death in most cases from respiratory failure. The death occurs within three to five years from diagnosis. Around 5 – 10% of patients have a family history of ALS and this form is thus sometimes referred to as familial or fALS. The rest of the cases are called sporadic or sALS. In the majority of ALS cases, the disease seems to be caused by the interaction of multiple genetic and environmental risk factors (Mead et al., 2023). So far, the only confirmed epidemiological risk factors correlated to ALS development are male gender and age (Longinetti and Fang, 2019). A genetic cause has been identified in 60 – 70 % of fALS patients (Ranganathan et al., 2020), but genetics also seem to play a role also in the absence of family history. More than 30 genes, either causative or associated with a higher risk of developing ALS, have been identified, with four of them accounting for 70 % of fALS cases – *chromosome 9 open reading frame 72 (C9orf72),superoxide dismutase (Sod1), TAR DNA binding protein (Tardbp), fused in sarcoma (Fus)* (Mead et al., 2023).

1.2 Glia in ALS

ALS does not only affect MNs but also other cell types. Glia have been shown to actively participate in the onset and progression of the disease (Boillée et al., 2006, Kang et al., 2013, Yamanaka et al., 2008).

Astrocytes become reactive during ALS, and it seems that the first signs appear even before the manifestation of symptoms and MN degeneration (Howland et al., 2002). Mutated SOD1 astrocytes from mice were shown to cause MN toxicity even before any reactive gliosis (Nagai et al., 2007) and astrocytes derived from sALS patients transplanted into the mouse also led to MN degeneration (Qian et al., 2017).

Beside their impact on neurons, astrocytes themselves have perturbed intracellular processes. There are reports of transcriptional deregulation of an immune response, lysosomal and phagocytic pathways or ion and cholesterol homeostasis (Baker et al., 2015, Miller et al., 2018). Downregulation of potassium channel Kir4.1 expression was detected in both SOD1 patients and rats (Kelley et al., 2018, Bataveljic et al., 2012) and murine SOD1 astrocytes were shown to have abnormal intracellular calcium dynamics (Kawamata et al., 2014). The perturbation of astrocyte´s homeostatic function could thus be an important factor during ALS.

Microglia, in the same way as astrocytes, become activated during ALS and their association with the disease has been known for a while. Hall et al. (1998) described some proinflammatory microglia detected in the mouse spinal cord before disease onset, whose number increased with disease progression, and they persisted into end-stage. When the activation was reduced, it extended the survival of mice (Martinez-Muriana et al., 2016).

The exact role, and especially the microglial heterogeneity during ALS, is associated with some contradiction. Originally, microglia´s contribution was thought to be important mostly later, during the progression, as the removal of the mutated gene from microglia caused lengthening of lifespan, but did not affect the onset point (Boillée et al., 2006). A study by Maniatis et al. (2019) using spatial transcriptomic in mouse spinal cord, however, showed that changes in microglial expression precede the changes in MNs, and another study reported a decreased number of microglia prior onset (Gerber et al., 2012). These thus suggest the involvement of microglia earlier in the disease process.

In pursuit of better microglia characterization, Keren-Shaul et al. (2017) used single-cell RNA sequencing and described a novel population called disease associated microglia (DAM). The population was originally described in a mouse model of Alzheimer´s disease, but they detected these microglia also in the spinal cord of SOD1(G93A) mice. They downregulate the homeostatic genes and simultaneously upregulate genes linked to inflammation, phagocytic and lipid

metabolism pathways. It seems that this subpopulation could be associated with clearance of the aggregates often accumulating during neurodegeneration, and the authors suggest that blocking microglia-specific checkpoints could be used therapeutically (Keren-Shaul et al., 2017, Yerbury et al., 2016).

Oligodendrocytes in the ALS mice model had a characteristically thickened cell body, they showed immunopositivity for the marker of apoptosis cleaved caspase-3 (CC3) and were surrounded by clusters of activated microglia (Kang et al., 2013, Philips et al., 2013). Demyelination of MN axons was reported in spinal cords of both SOD1(G93A) mice as well as in ALS patients. Consistently, myelin basic protein (MBP) levels were reduced in the spinal cord of SOD1(G93A) mice (Philips et al., 2013).

Neuroinflammation is generally associated with microglia, but it affects the functioning of oligodendrocytes in ALS as well. They can react to inflammation through the expression of cytokines, inflammasomes and chemokines, which make them along with astrocytes and microglia active in the neuroinflammatory network (Zeis et al., 2016).

1.3 Alzheimer´s disease

Alzheimer´s disease (AD) is a progressive neurodegenerative disorder affecting an ever-increasing number of people and is the main cause of dementia (Scheltens et al., 2021). The degeneration strikes mainly in the prefrontal, entorhinal cortex and hippocampus, which are structures associated with learning and memory, and further linked to the limbic system, thus cognitive and emotional processes (Minati et al., 2009, Kulijewicz-Nawrot et al., 2012). Most cases occur after the age of 65, but in some cases, the onset can be early. AD is generally associated with some biological hallmarks such as extracellular accumulation of amyloid β (Aβ), tau accumulation (Duyckaerts et al., 2009), glial pathology, and disruption of ion homeostasis among others.

Back in 1910, A. Alzheimer reported pathologically modified astrocytes and discovered the abundance of glia near the neuritic plaques (Tagarelli et al., 2006). Later on, astrogliosis became known as a typical morphological feature of AD brains and was detected in human patients as well as in AD animal models (Nagele et al., 2004, Nagele et al., 2003, Rodriguez et al., 2009, Olabarria et al., 2010). Aβ seems to also affect the physiological properties of astrocytes. Beside calcium signaling (Abramov et al., 2003, Abramov et al., 2004), their homeostatic functions are impaired. This affects the glutamate and overall ion homeostasis (Ben Haim et al., 2015, Hynd et al., 2004).

2 OBJECTIVES

Hypothesis 1.: Cortical glial cells are affected by the ALS pathology in patients, however, the data from the SOD1(G93A) mice model are contradictory. Some studies reported a decreased number of neurons and signs of gliosis (Miller et al., 2018, Gomes et al., 2019, Migliarini et al., 2021), while others suggested that the cortical pathology is limited to the spinal cord (Niessen et al., 2006). We hypothesize that the changes in cortical glia may be minimal and thus difficult to detect. Therefore, the use of advanced methods such as sequencing on a single cell level can bring better insights into the discussion.

Aim 1.: To assess the extent to which cortical glia are affected by the ALS-like pathology in the SOD1(G93A) model of ALS.

Hypothesis 2: Multiple studies describe the potential pathological or neuroprotective roles of astrocytes in ALS (reviewed in You et al. (2023)). However, despite astrocytes being the primary homeostatic cells in the CNS, there is insufficient information about their homeostatic functions throughout the disease progression. Although there are reports of potassium channel downregulation in the SOD1(G93A) model, studies on the functional impact of this downregulation are lacking. Additionally, potential discrepancies exist between animal models with different genetic backgrounds. We hypothesize that the pathology impairs the ability of astrocytes to maintain ion homeostasis, which in turn can influence the CNS environment and disease progression.

Aim 2.: To unveil the astrocytic capacity to regulate ion homeostasis in the cortex and spinal cord of SOD1(G93A) model on the FVB/N background.

Hypothesis 3.: Under pathological conditions, the ion concentration in the extracellular space (ECS) increases significantly (Pasantes-Morales and Vazquez-Juarez, 2012). Astrocytes physiologically sustain the homeostasis; however, like other cell types, aging can cause a loss/alteration of their normal functions (Palmer and Ousman, 2018). Such change can then add to the progression of AD. We hypothesize that the ability of astrocytes to regulate their volume will decline with

age and the progression of AD. Related to that, we expect changes in the composition and structure of the extracellular matrix (ECM) associated with changes in astrocytic volume and morphology. Analysis of astrocytes and ECM at different time points throughout the AD progression will shed more light on aging as an additional risk factor affecting the disease.

Aim 3.: To characterize the astrocytic ability to control ion uptake and characterize the extracellular composition in the AD mouse model.

3 MATERIALS AND METHODOLOGY

3.1 Animals

As a model of ALS, we used transgenic mice expressing high levels of human SOD1(G93A) (JAX Strain: 004435 C57BL/6 J-Tg (SOD1*G93A)1Gur/J) and their non-carrier littermates (Gurney et al., 1994). Additionally, we crossbred the SOD1 males and the GFAP/EGFP (Nolte et al., 2001) females to obtain a model of ALS with fluorescently labeled astrocytes due to the expression of enhanced green fluorescent protein (EGFP) under the control of the human glial fibrillary acidic protein (GFAP) promoter. Similarly, we generated a crossbreed by breeding a triple transgenic model of AD, containing three mutations associated with familial AD (APP Swedish, MAPT P301L, and PSEN1 M146V) (Oddo et al., 2003) and GFAP/EGFP strain (Nolte et al., 2001) for the analysis of astrocytes in the AD model.

3.2 Behavioral testing

Two types of motor tests were conducted - the wire grid hang test and the Rotarod test to assess muscle strength, function, and coordination throughout the disease. Testing consisted of one three-attempt session every week. All animals performed training beforehand. During the wire grid hang test the mouse was placed on a custom-made wire lid, approximately 60 cm above a wood chip covered bottom, and the lid was turned upside down. The Rota-rod testing comprised of the mouse being placed on a stationary rod facing against the direction of rotation. The rod rotation was set to a constant speed of 15 rpm. In both cases, we measured the latency to fall.

3.3 Preparation of acute brain and spinal cord slices

Mice were deeply anesthetized and transcardially perfused with a cold isolation buffer. Brain and spinal cord were dissected. Coronal slices (300 μm for 3D-morphometry and 400 μm for the TMA method) were cut and then incubated. After

the incubation, they were kept at room temperature in artificial cerebrospinal fluid (aCSF).

3.4 Three-dimensional confocal morphometry

The volume changes of astrocytes were studied using 3D morphometry in acute tissue slices. Tissue slices were placed into the recording chamber and held down with a U-shaped platinum wire. The chamber was continuously perfused with recording solutions. All measurements were performed at room temperature using a confocal microscope with a 60× LUMPLFLN water immersion objective. The cells were captured as a series of two-dimensional (2D) sectional images. During the cell volume changes induced by various solution treatments, individual 3D images were acquired at 5-minute intervals, 4 times in total. The cell volume recovery was checked after 20 and 40 minutes. Image processing and morphometric analysis were carried out using Cell Analyst software and ImageJ.

3.5 Real time iontophoretic method

Slices were placed in the chamber connected to Zeiss Axioscope and manipulators. Measurements were performed at room temperature in a depth of 200 μm. The TMA^+ was put into the tissue through the iontophoretic micropipette and the diffusion was measured by double-barreled ion-selective microelectrodes. The diffusion curves were analyzed using the VOLTORO program (kindly provided by C. Nicholson, New York University School of Medicine, USA, unpublished data) to acquire the parameters, which are volume fraction α, tortuosity λ and nonspecific uptake k'.

3.6 Preparation of single-cell suspension

Mice were deeply anesthetized and transcardially perfused. The motor cortex was isolated and processed according to the Adult Brain dissociation protocol for mice and rats (Milteyni-Biotec, Germany) with the addition of actinomycin D to prevent activation of immediate early genes. The final suspension was labeled with ACSA-

2, Cd11b and O4 antibodies conjugated with allophycocyanin and phycoerythrin respectively. Cell types were enriched using fluorescence activated cell sorting (FACS). Four animals per condition were pooled for the preparation of cell suspension.

3.7 Single cell RNA-Sequencing

We used Chromium Next GEM Single Cell 3' Reagent Kits v3.1 to prepare the sequencing libraries, and the protocol was performed according to the manufacturer's instructions. The concentration and quality of the libraries was measured, and the libraries were pooled and sequenced in paired-end mode using Illumina NovaSeq 6000 SP Reagent Kit.

3.8 RNA-Sequencing data analysis

To analyze the sequencing data, we used differential expression (DE) analysis and gene set enrichment analysis (GSEA). To examine the individual cell types of interest, we used principal component analysis.

3.9 Immunohistochemistry and confocal microscopy

Immunohistochemical analysis was used to evaluate the morphology of glial cell types, apoptosis, myelination and channel expression in ALS animals (Table 1). Cell nuclei were visualized by DAPI staining (Merck, Darmstadt, Germany). Confocal fluorescence microscopes together with ImageJ software were used for the analysis of fluorescence signals.

Table 1: Primary antibody used for immunohistochemistry

Targeted cell type/structure	Antibody	Species	Dilution	Company
Myelin	MBP	rat	1:500	Biorad
Microglia	Iba-1	rabbit	1:500	Abcam
Apoptotic cells	CC-3	rabbit	1:50	CellSignaling
Oligodendrocytes	APC	mouse	1:200	Merck

Astrocytes	ALDH1L1	rabbit	1:500	Abcam
Kir4.1 channel	Kir 4.1	guinea pig	1:300	Alomone

3.10 Cerebrospinal fluid (CSF) isolation and elemental analysis

To isolate the cerebrospinal fluid, we used modified protocol (from Kaur et al., 2023). The mice were first anesthetized with 3% isoflurane (Abbot, IL, United States) and maintained at 1-2% isoflurane using a vaporizer (Tec-3, Cyprane Ltd., Keighley, United Kingdom). We did not use a stereotactic instrument but followed the protocol with cisterna magna exposure and then the CSF extraction. We looked for any traces of blood contamination and used only clear samples for further analysis (Fig. 8). The mice were sacrificed immediately after the experiment.

The ion concentration in the cerebrospinal fluid was determined using inductively coupled plasma optical emission spectroscopy (ICP-OES) coupled with an electrothermal evaporation (ETV) unit in the analytical laboratory at IOCB Prague.

3.11 Statistics

All results are expressed as the mean ± standard error of the mean (SEM). Values of $p < 0.05$ were considered significant, $p < 0.01$ very significant and $p < 0.001$ extremely significant.

4 RESULTS

4.1 Characterization of the SOD1(G93A) mouse model phenotype and pathological traits in the motor cortex

To explore the cellular pathology in the cortex, we employed scRNA-Seq. We performed DEA to investigate ALS-related transcriptional changes. The *Sod1* gene was the only significantly upregulated DEG in all measured stages of the disease. Other dysregulated genes were mostly noncoding or ribosomal transcript that evaded quality control. Altogether, our results showed minimal gene expression variation related to ALS progression in the cortex of SOD1 animals regardless of sex, but with indication of some changes in microglia and oligodendrocytes at the end-stage of the disease.

We speculated that the minor changes might be represented by a small fraction of cells. To explore this, we used an in-depth sub-clustering analysis with the goal to identify subpopulations potentially playing a role in the disease.

The analysis of astrocytes revealed three clusters present in both CTRL and SOD1 samples in similar proportions (Fig. 1a) and the results generally revealed no changes or presence of a SOD1-specific subpopulation.

Microglia were grouped into four clusters (Fig. 2b). Cluster 1 was marked by the expression of homeostatic genes (Butovsky and Weiner, 2018, Keren-Shaul et al., 2017, Mathys et al., 2017). The signature of clusters 2 and 3 resembled the expression profile of ARMs and the number of cells was slightly increased in SOD1. Cluster 4 was clearly marked by the expression of genes involved in the interferon response pathway and thus represented IRMs (Sala Frigerio et al., 2019). The IRM proportion though, was very low in both conditions.

Oligodendrocytes formed four clusters (Fig. 1c). Cluster 1 represented forming oligodendrocytes (MFOL) described by Marques et al. (2016). Cluster 2 represents mature oligodendrocytes (MOL2). Clusters 3 and 4 had increased expression of several genes detected in mature oligodendrocyte populations MOL5/6 (Floriddia et

al., 2020, Marques et al., 2016). Strikingly, cluster 4 was almost exclusively present in the SOD1 samples (Fig. 1d). It was characterized by a higher expression of the genes mentioned in association with disease-associated oligodendrocytes (Kenigsbuch et al., 2022, Lee et al., 2021), immune oligodendroglia, multiple sclerosis, and chronic demyelination (Jakel et al., 2019) and we thus hypothesize that cluster 4 could be damaged or reactive oligodendrocytes, reacting to the pathological processes in the SOD1 cortex.

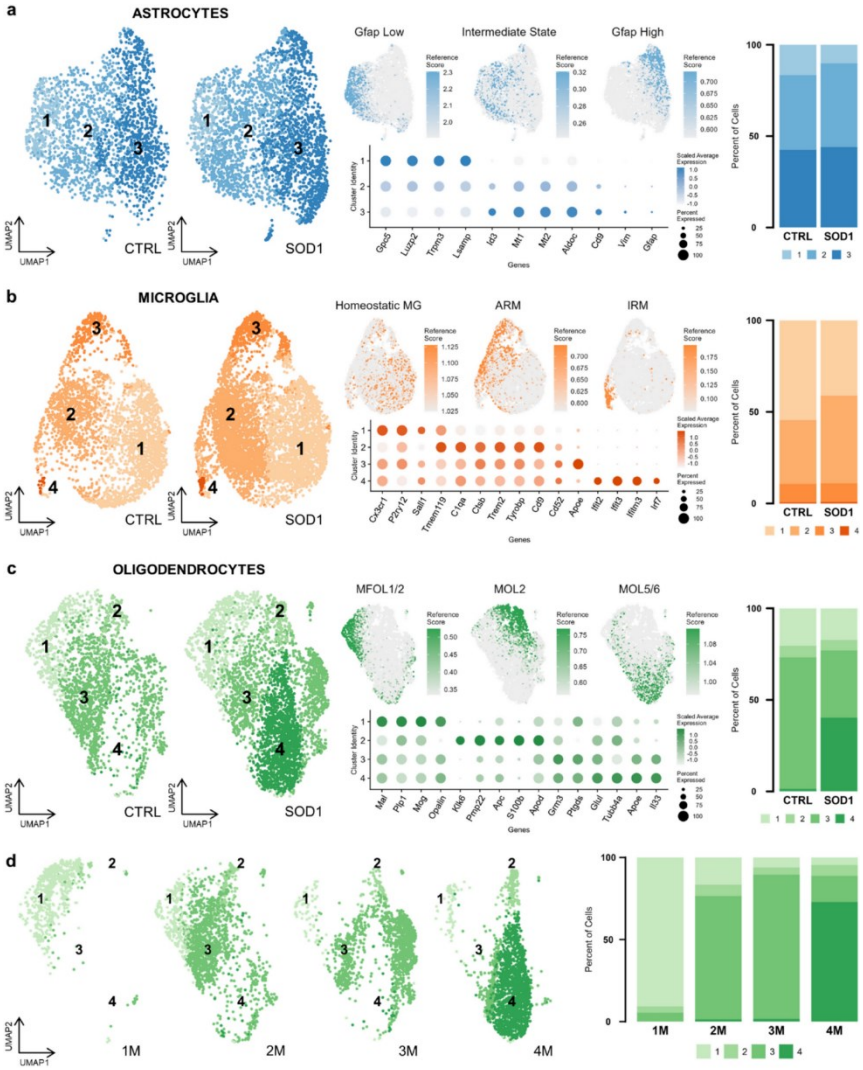

Figure 1 The subpopulation analysis revealed a unique subpopulation of oligodendrocytes in SOD1 samples. UMAP visualization of subpopulations of astrocytes (n = 5292) A), microglia (n = 8414) B), and oligodendrocytes (n = 5876) C) split to CTRL and SOD1 condition (left), including cells from all four time points. Gene expression signatures of previously described subpopulations are shown projected onto UMAP (middle-top). A list of representative cluster markers used for their annotation (middle-bottom). Proportions of subpopulations in CTRL and SOD1 (right), including cells from all four time points. D) UMAP visualization of CTRL and SOD1 oligodendrocytes split according to age (1 m: n = 682, 2 m: n = 1697, 3 m: n = 1430, 4 m: n = 2067). Bar plot shows proportions of subpopulations at each time point.

To validate the conclusions from the scRNA-seq, we used immunohistochemical analysis of glia in the motor and primary somatosensory cortex (the identical region used for the sequencing) (Fig. 2a).

In astrocytes, we looked for signs of astrogliosis. The fluorescence analysis showed similar fluorescence values of both CTRL and SOD1 slices, suggesting no morphological changes associated with activation (Fig. 2b, c).

To study the morphology of microglia, we used the IBA1 antibody and Sholl method. Results from this analysis confirmed that the morphology of CTRL and SOD1 microglia did not differ (Fig. 2d). However, we identified *bulbous termini*, which appear as the first reaction of microglia after injury (Davalos et al., 2005) (Fig. 2e).

The cells in cluster 4 of oligodendrocytes could be damaged due to pathology and we thus focused on the protein expression changes related to chronic demyelination, necrosis or apoptosis. We stained for myelin basic protein (MBP)—a marker of myelination, adenomatous polyposis coli (APC)—a marker of adult oligodendrocytes, and cleaved caspase 3 (CC3)—an apoptotic marker. The quantification of MBP excluded the hypothesis of demyelination processes as there was no decrease of MBP or APC+ cells in the SOD1 compared to CTRLs (Fig. 2f). Similarly, the co-staining of CC3+ oligodendrocytes suggest a similar rate of apoptosis for both CTRL and SOD1 (Fig. 2f). Overall, the data did not show significant demyelination or degeneration, and it is thus likely, that cluster 4 does not represent dying or damaged cells.

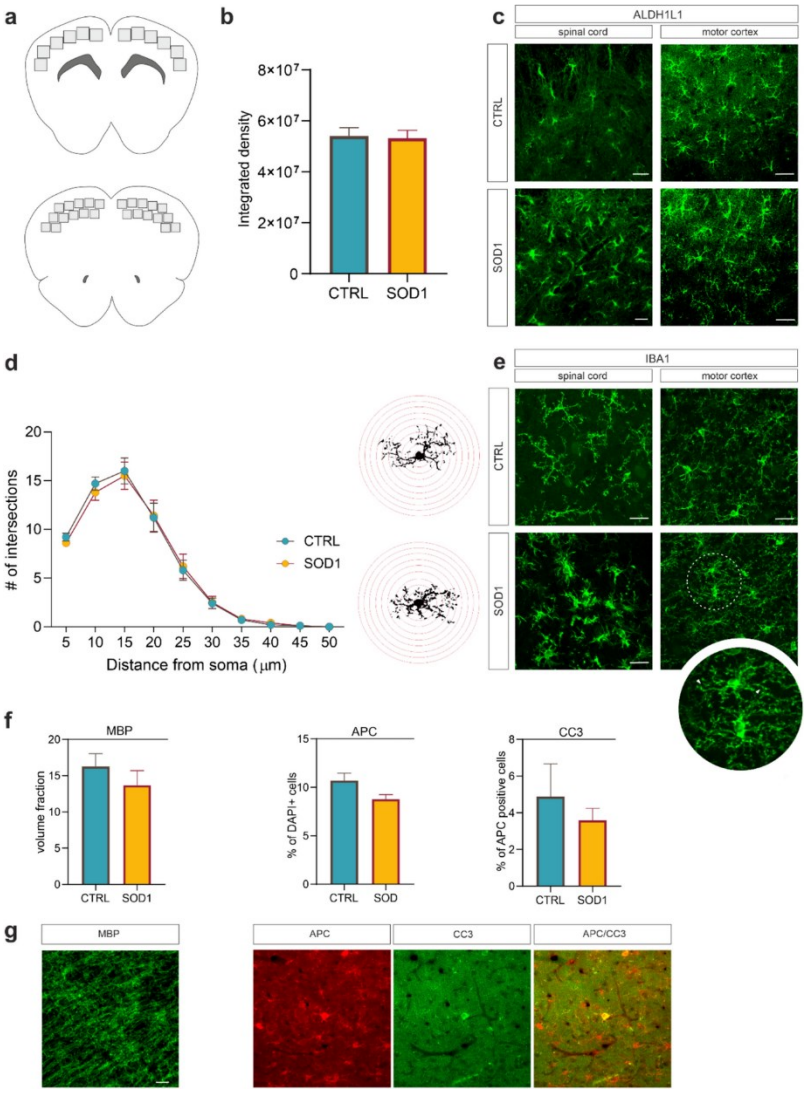

Figure 2 The immunohistochemistry A) The upper cartoon depicts 12 areas scanned for the investigation of morphological changes and quantification of APC and CC3. The lower cartoon shows 24 areas scanned for the MBP analysis. B) Fluorescence analysis did not reveal any significant differences in morphology between cortical astrocytes in SOD1 (n = 6) and CTRL (n = 6) animals. C) Representative pictures of ALDH1L1 staining in the cortex and spinal cord comparing astrocytes, showing morphological difference between SOD1 and CTRL in the spinal cord but no noticeable difference in the cortex. D) The results of Sholl analysis indicated very similar microglia complexity in both CTRL (n = 6) and SOD1 (n = 6) samples. Sholl masks with red concentric radii depict single threshold microglia as they were used for the analysis. E) Representative images of cortical and spinal slices stained with IBA1 show evident amoebic morphology of spinal microglia, but only subtle morphological changes represented by *bulbous termini* (see close-up) in the cortex. F) The quantification of MBP in the cortex revealed insignificant difference between SOD1 (n = 6) and CTRLs (n = 6). The number of APC+ cells was consistent between SOD1 (n = 3) and CTRLs (n = 3) and the number of APC+ cells co-stained with CC3 used as a marker of apoptosis in oligodendrocytes also remained similar, suggesting no apparent oligodendrocyte degenerations. G) Representative images of MBP, APC, and CC3 staining scale bars, 20 μm. The statistical significance was determined using unpaired t-test. Data are presented as mean ± SEM. N states the number of animals used.

4.2 Functional properties of astrocytes in a mouse model of ALS

To assess the functional properties of astrocytes, we generated a crossbred animal with ALS-like pathology and fluorescently labeled astrocytes (Nolte et al., 2001). To confirm the phenotype of the SOD1/GFAP/EGFP mice, we used the wire grid hang test and Rotarod.

Our findings confirmed that the crossbred mice exhibit classic ALS symptoms (Fig. 3). Interestingly, we found notable differences in the performance during the symptomatic stage (Fig. 3c, d) when comparing our crossbreed with the original SOD1/C57Bl6. Motor coordination, assessed by the Rotarod test, was also more severely affected in SOD1/GFAP/EGFP mice (Fig. 3d).

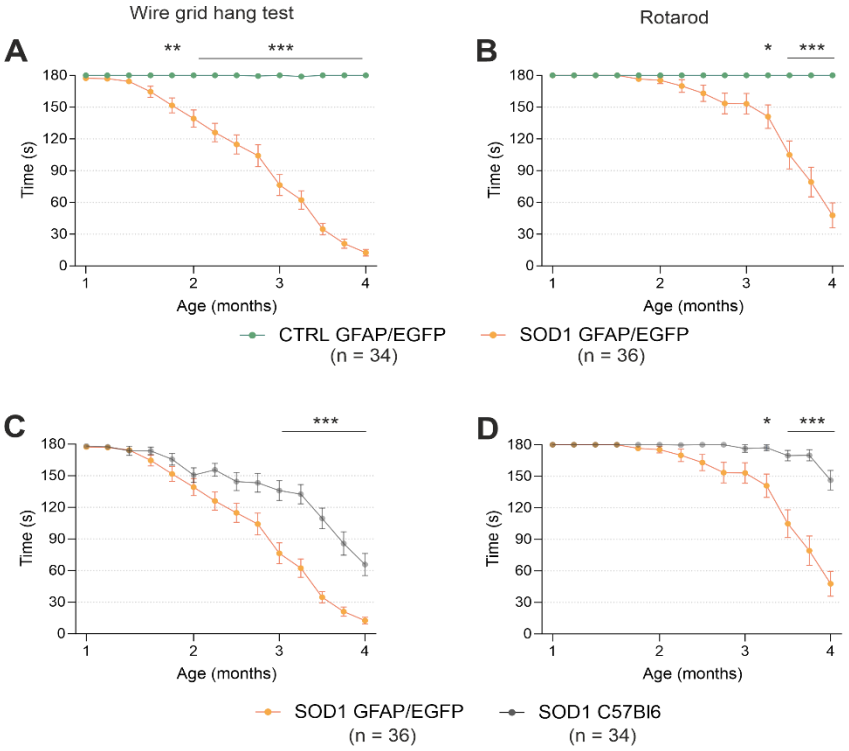

Figure 3 Behavioral testing A) the Hanging wire test confirmed the motor strength decline in SOD1/GFAP/EGFP mice compared to CTRLS. B) Rotarod measurements analysis revealed the decline of motor coordination in SOD1/GFAP/EGFP mice compared to CTRLS and thus confirmed the phenotype. C) Comparison of motor strength revealed significantly faster progression in SOD1/GFAP/EGFP mice compared to the initial SOD1/C57BL6. D) Similar trends were observed in Rotarod results, showing a faster decrease of motor coordination in sod1 GFAP/EGFP mice. Data are presented as mean ± SEM. n = the number of mice.

As we were interested in astrocytes, we were also looking for signs of astrogliosis. We took advantage of the eGFP-labeling and performed fluorescence analysis in the motor- the somatosensory cortex, and the ventral horns of the lumbar spinal cord.

The results from the motor and somatosensory cortex (Fig. 4a) revealed a significantly larger fluorescent area in the SOD1 mice, and we observed the same situation in the ventral horns of the lumbar spinal cord (Fig. 4b). This data suggests a higher GFAP positivity (thus a visible change in morphology and/or increase of GFAP-positive cells) caused by ALS-like pathology, which confirms that astrocytes are activated in both the brain and spinal cord during the disease progression in the model on the FVB/N background.

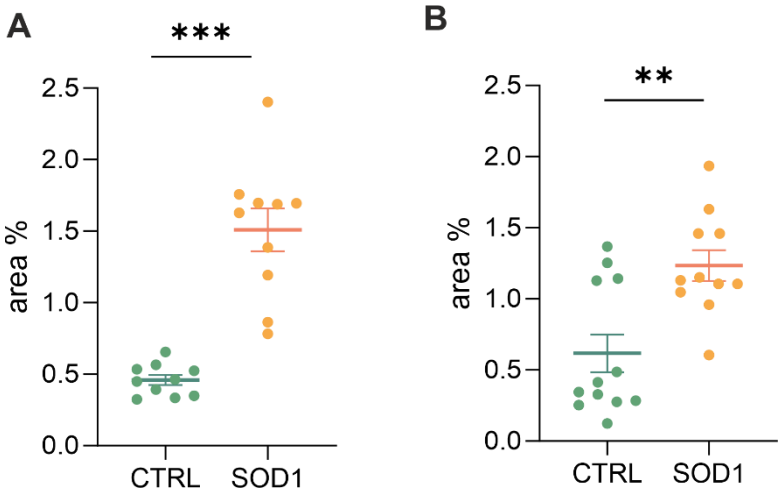

Figure 4 Assessment of astrocyte reactivity based on GFAP expression levels A) representative tile scans of motor cortex used for fluorescence analysis. The SOD1 cortex shows signs of astrogliosis. B) Fluorescence analysis of astrogliosis in the motor and somatosensory cortex of sod1 and ctrl mice showed astrogliosis in SOD1 mice. C) Representative pictures of astrocytes in the ventral horns of the spinal cord. D) Fluorescence analysis of astrogliosis in the spinal cord confirmed a gliosis and morphological shift of astrocytes towards the reactive shape. Data are presented as mean ± SEM. n = the number of brain hemispheres or spinal cord slices, respectively. CTRL, control mice on the FVB/N background; SOD1, superoxide dismutase transgenic mice on the FVB/N background

In addition to morphology, we were interested in the Kir4.1 expression (Fig. 5a) as it is, among other factors, responsible for regulating K^+ homeostasis in cells. We examined the protein expression in the motor and the somatosensory cortex as well as in the spinal ventral horns. Our results show that there is no significant difference between Kir4.1 expression in the cortex, as the obtained values were almost equal in both SOD1 and CTRL mice (Fig. 5b). However, the analysis in the ventral horns revealed significant downregulation of the Kir4.1 channel (Fig. 5c).

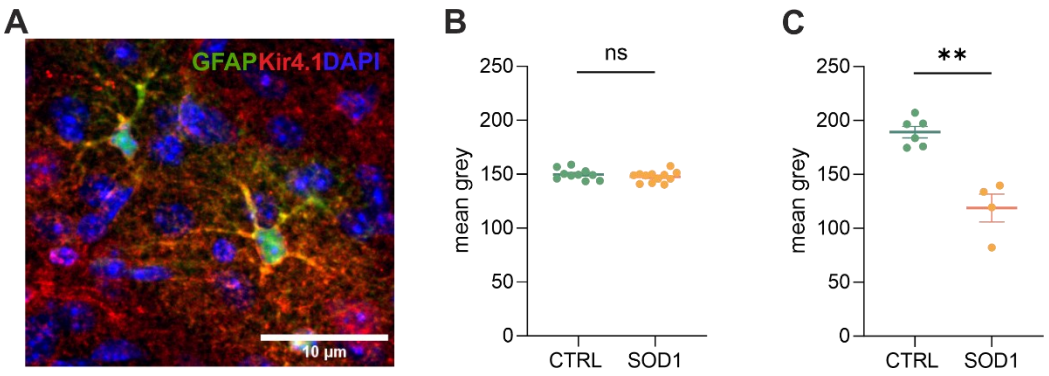

Figure 5 Immunohistochemical analysis of Kir4.1 expression A) a representative picture of Kir4.1 staining in the motor cortex. B) Fluorescence analysis of Kir4.1 in the primary and secondary motor cortex and somatosensory cortex. C) Fluorescence analysis of Kir4.1 in the ventral horns of the spinal cord. Data are presented as mean ± SEM. n = the number of brain hemispheres or spinal cord slices, respectively. CTRL, control mice on the FVB/N background; SOD1, superoxide dismutase transgenic mice on the FVB/N background.

The immunohistochemistry revealed morphological changes in both cortical and spinal astrocytes suggesting their shift toward an activated state and Kir4.1 downregulation in the ventral horns of lumbar spinal cord of SOD1 mice. We were interested to see whether these changes will correlate with astrocytic swelling during hyperkalemia. We used 20 mM and 50 mM $aCSF_{K+}$ solutions to simulate elevated potassium levels occurring e.g. during closed brain injury and ischemia, respectively (Rossi et al., 2007, Muller and Somjen, 2000, Pietrobon and Moskowitz, 2014).

Despite the observed astrogliosis in the brain, the measurements and following data analysis revealed that SOD1 cortical astrocytes can handle higher potassium levels with the same efficacy as healthy astrocytes during both 20 and 50mM K^+ application (Fig. 6b, c). Spinal astrocytes have unimpaired buffering ability in the 20 mM K^+ environment (Fig. 6d) but during the application of the 50 mM $aCSF_{K+}$ swelled significantly less than the CTRL astrocytes at each measured time point during the application (Fig. 6e). The diminished swelling in the high potassium environment suggests inefficient buffering of the extracellular potassium level and a potential potassium homeostasis imbalance in the SOD1 spinal cord.

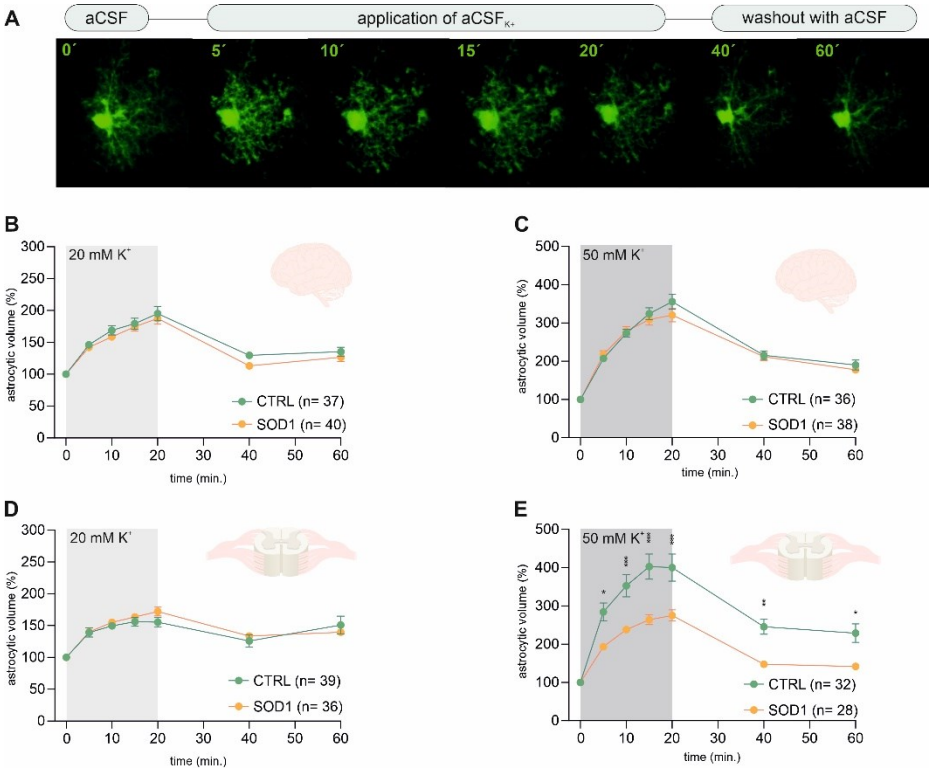

Figure 6 Swelling of astrocytes in response to different potassium concentrations A) superimposed confocal images of an eGFP-labeled cortical astrocyte recorded throughout the measurement. B, C) the time course of volume changes of cortical (B) and spinal (C) astrocytes throughout the measurement in 20mm aCSF$_{K+}$. (D, E) time course of volume changes of cortical (D) and spinal (E) astrocytes throughout the measurement in 50mm aCSF$_{K+}$. Data are presented as mean ± SEM. n = number of cells. CTRL, control mice on the FVB/N background; SOD1, superoxide dismutase transgenic mice on the FVB/N background.

To investigate alterations in the dynamics of the ECS diffusion properties, we used the real-time iontophoretic (RTI) method in the brain and spinal cord. We hypothesized that the alterations in astrocyte morphology and their functional properties detected by 3D-morphometry could also be manifested as variations in the ECS parameter values. We quantified volume fraction (α) and tortuosity (λ).

Application of 20mM and 50 mM aCSF$_{K+}$ on brain slices induced cell swelling leading to a shrinkage of the ECS volume, manifested as a compensatory decrease of the ECS volume fraction, but we did not identify any significant differences between SOD1 and CTRL animals. Tortuosity values remained unchanged.

Exposure of the spinal cord tissue to 20mM aCSF$_{K+}$ caused volume fraction decrease but it did not differ between the groups (Fig. 7a, b). Exposure to 50mM aCSF$_{K+}$ on

the other hand resulted in a significantly more profound decrease in the ECS volume fraction in CTRL compared to SOD1 mice (Fig. 8c). Tortuosity values remained unchanged (Fig. 8d).

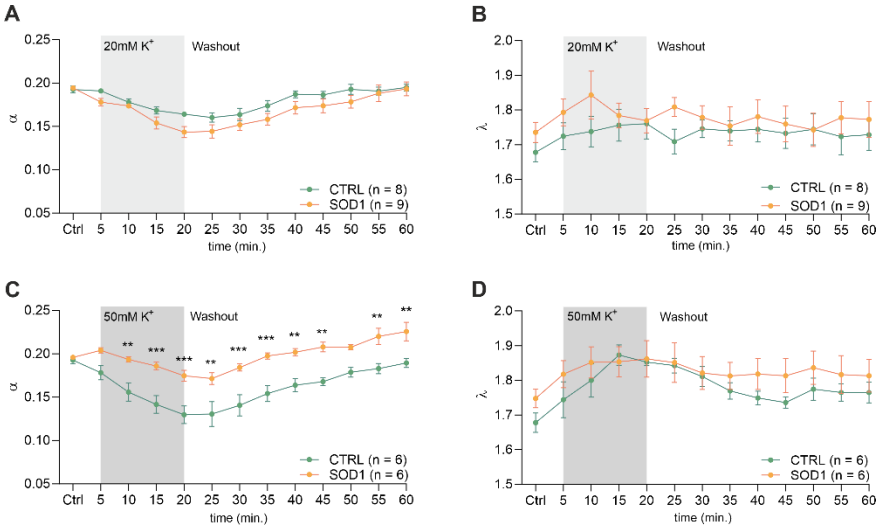

Figure 7 Measurements of ECS in acute spinal cord slices averaged data of α – volume fraction and λ - tortuosity measured in CTRL and SOD1 mice at resting conditions (22-24°c, CTRL), and at 5-minute intervals during application of 20mm (A) and 50mm (B) $aCSF_{K+}$ and washout (aCSF). Data are presented as mean ± sem. n = the number of slices. Ctrl, control (initial measurements); CTRL, control mice on the FVB/N background; SOD1, superoxide dismutase transgenic mice on the FVB/N background.

The data from functional measurements and immunohistochemical analysis suggested that the SOD1/GFAP/EGFP mice could suffer from potassium imbalance. To determine the extracellular potassium concentration and reveal possible deregulation, we used elemental analysis. In addition to potassium, we analyzed Ca, Fe, Mg, Na, P and S. The potassium concentrations were comparable between SOD1 and CTRLs (Fig. 8b) and both were within the range of the physiological concentration. Interestingly, we detected a significantly lower concentration of magnesium in the CSF of SOD1 mice (Fig. 8c). Magnesium is, among others, involved in muscle function and neuronal signaling, and a lower magnesium concentration was reported in a post mortem analysis of ALS patients previously (Yasui et al., 1997).

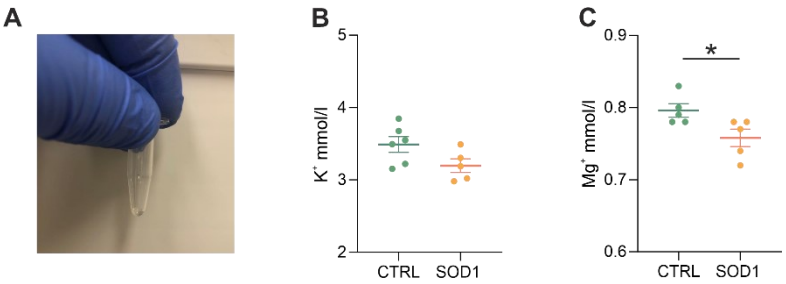

Figure 8 Elemental analysis of CSF isolated from GFAP/EGFP mice A) a sample of CSF demonstrating the purity of all samples used for the analysis. B) A comparison of potassium concentrations in the CSF of control vs. SOD1 mice. C) A comparison of magnesium levels in the CSF of control vs. SOD1 mice. Data are presented as mean ± SEM. n = the number of mice. CTRL, control mice on the FVB/N background; SOD1, superoxide dismutase transgenic mice on the FVB/N background.

4.3 Astrocyte swelling during hyperkalemia in a model of AD

We tested the ability of astrocytes to regulate their volume and swell in acute brain slices from 3M, 9M, 12M and 18M mice exposed to either hypotonic solution ($aCSF_{H-100}$) to evoke a hypo-osmotic stress or a potassium solution ($aCSF_{K+}$) to evoke a severe hyperkalemia.

We did not observe any age-dependent cell volume variations in response to hyperkalemia or hypo-osmotic stress, however, we discovered that astrocyte swelling caused by both hypo-osmotic stress and hyperkalemia was lower in the 3xTg-AD animals than in their age-matched controls.

We also performed measurements of the extracellular diffusion parameters in the CA1 region of hippocampal slices using the RTI method. Physiological aging was accompanied by a decrease in volume fraction, while this tendency was lost during AD. However, an increase in the number of obstacles (tortuosity) occurred earlier in AD than in physiological aging. Changes in volume fraction and tortuosity evoked by hypo-osmotic stress were comparable between the 3xTg-AD mice and their age-matched controls. The changes in ECS volume fraction and tortuosity evoked by hyperkalemia were comparable within 3 – 12M of age.

5 DISCUSSION

5.1 Characterization of the SOD1(G93A) Mouse Model Phenotype and Pathological Traits in the Motor Cortex

The SOD1(G93A) stands out as the most used and thoroughly characterized mouse model in ALS research. However, despite its extensive use, the effect of pathological changes across different CNS regions remains incompletely understood. A study by Ozdinler et al. (2011) and others reported early cortical motor neuron degeneration, along with changes in glial cells (Miller et al., 2018, Gomes et al., 2019, Migliarini et al., 2021). Additionally, some studies have suggested that pathology in the SOD1 model is restricted to spinal and bulbar motor neurons, not affecting the motor cortex at all (Niessen et al., 2006). These conflicting findings raise questions about the extent to which the cortex is affected in the SOD1 mouse model and how accurately this model represents the cortical pathology ongoing in humans.

The single-cell profiling focused on glial cells revealed minor changes in microglia and oligodendrocytes, but no significant ALS-related shifts in astrocytes, which contrasts with several studies that reported a reactive astrocyte phenotype (Miller et al., 2018, Gomes et al., 2019, Gomes et al., 2020).

Our data generated within the motor and primary somatosensory cortex regions, representing the end-point of the corticospinal tract affected by ALS, allowed us to also address questions regarding the site of origin and direction of ALS progression. Considering the advanced ALS-like phenotype in end-stage SOD1 mice accompanied by more pronounced changes observed in the brainstem and spinal cord, the milder cortical changes indicated by our data support the ‘dying back’ hypothesis in SOD1(G93A) mice proposing that ALS begins within muscles or neuromuscular junctions.

Recent seminal studies using scRNA-seq have identified various disease-associated glial populations that play significant roles in disease progression (Keren-Shaul et al., 2017, Sala Frigerio et al., 2019, Habib et al., 2020, Falcao et al., 2018).

We searched for these populations, but without success, which confirms the minimal changes observed at the bulk transcriptional level and by immunohistochemistry. However, the sub-clustering analysis revealed a unique population of oligodendrocytes characterized by increased expression of *Apoe* and *Il33*, specifically enriched in 4-month-old SOD1 samples. Considering the absence of significant oligodendrocyte loss or higher apoptotic rates in immunohistochemistry, we speculate about the active role of this oligodendrocyte population in disease progression. This would align with recent evidence suggesting an active role of oligodendrocytes in the progression of multiple sclerosis (Falcao et al., 2018) and in aging white matter (Kaya et al., 2022), which contrasts with their traditionally perceived passive role.

5.2 Functional Properties of Astrocytes in a Mouse Model of ALS

To understand how ALS affects astrocytic functional properties, we generated a mouse on the FVB/N background with ALS-like symptoms and fluorescently labeled astrocytes. The different backgrounds or point mutations seem to cause variability in phenotype and certainly, our behavioral testing revealed notable differences in disease progression between the original SOD1, which has the C57Bl6 background model and our crossbreeds. Prior studies have shown that various ALS models exhibit phenotypic variations affecting disease progression, possibly due to factors such as microglia-mediated neuroinflammation (Heiman-Patterson et al., 2011, Nikodemova and Watters, 2011) or metabolic hyperactivity.

While astrocytic activation in the spinal cord is expected and is well-documented in the original SOD1/C57Bl6 model (Baker et al., 2015, Nagai et al., 2007), cortical astrocytes remain controversial. To the best of our knowledge, no studies have examined astrocyte activation in the SOD1 model on an FVB/N background, limiting direct comparisons. However, given the faster disease progression observed in our model, it is possible that the astrogliosis was more pronounced and thus easier to detect than in the animals on the C57Bl/6 background.

The swelling reflects astrocytic ability to uptake K^+, which contributes to maintaining the potassium homeostasis. Recently, studies have reported a reduced potassium clearance rate in the motor cortex of SOD1/C57Bl6 mice, correlating with motor neuron loss (Ding et al., 2024, Stevenson et al., 2023). However, our data revealed comparable swelling in both control and SOD1 cortical astrocytes, suggesting that potassium uptake remains intact in the cortex of SOD1/GFAP/EGFP mice despite significant astrogliosis. The uptake is however, only one of the intricate clearance mechanisms. Recently, Stevenson et al. (2023) proposed a possible interpretation of the divergence in our data. They explain the reduced clearance by reduced coupling of astrocytes, which prevents spatial buffering rather than by a changed K^+ uptake. The uptake is closely associated with the potassium channels and ion transporters. The pivotal channel responsible for K^+ removal is Kir4.1. This is expressed primarily in astrocytes and their altered expression has been previously reported in SOD1(G93A) rats and mice (Bataveljic et al., 2012, Kaiser et al., 2006) in the spinal cord but not in the cortex. This aligns with our results from immunohistochemistry, showing no difference in Kir4.1 expression in the cortical astrocytes and we associate this with the non-different swelling.

A comparison between the RTI measurements and analyses of astrocytic swelling revealed similar responses to increased K^+ levels. As noted in earlier studies, such consistency between RTI and 3D morphometry results is rare, given that RTI captures volume changes across all cell types, not just astrocytes (Kolenicova et al., 2020, Tureckova et al., 2021). These findings highlight the pivotal role that astrocytes play in hyperkalemia-induced cell swelling.

In addition to K^+, other ions, such as Ca^{2+} (Alexianu et al., 1994), Na^+ (Kuo et al., 2004, Kuo et al., 2005, Pieri et al., 2009), and Mg^{2+}, are also dysregulated in ALS. We examined the CSF and we only found a notable decrease in magnesium levels in SOD1 mice. Magnesium is crucial for muscle function, cellular antioxidant mechanisms, and neuronal signaling, particularly in preventing excitotoxicity by inhibiting NMDA receptors (Shindo et al., 2020). The decrease we revealed aligns

with previous findings in postmortem samples from ALS patients (Yasui et al., 1997), suggesting that magnesium deficiency could be a potential risk factor for ALS.

5.3 Functional Properties of Astrocytes in the Model of Alzheimer´s Disease

ALS and AD share some pathways of neurodegeneration, although manifested in different clinical symptoms, and we inspected the astrocytic functional properties also in AD.

The AD mice exhibited lower volume changes than CTRLs, and these changes were consistent across different age groups. These findings suggest that mechanisms for the uptake or extrusion of osmotically active substances, such as ions and neurotransmitters, as well as water transport, are impaired in 3xTg-AD mice. We hypothesized that these defects could stem from altered expression of channels and transporters.

Unlike physiological aging, we observed no age-related decline in volume fraction in 3xTg-AD mice. This result aligns with findings from another AD model, APP23 mice (Sykova et al., 2005), and could be linked to amyloid deposits in the ECS, which would prevent the reduction of ECS volume in aged tissue.

The comparison of tortuosity revealed more hindered extracellular diffusion (higher λ values) in the 12M 3xTg-AD mice compared to age-matched controls. Some studies showed (Roitbak and Sykova, 1999, Vegh et al., 2014, Zamecnik et al., 2004) that during various pathological conditions, the increase in ECS volume and/or tortuosity are aligned with the ECM overexpression. Conversely, the decrease in those values is associated with decreased ECM content or lack of core ECM molecules (Bekku et al., 2010, Sykova et al., 2005).

6 CONCLUSIONS

In the presented work, we focused on the role and involvement of glial cells in ALS mouse models and then further inspected the astrocytes also in a model of AD as they share some pathological features. We used multiple animal models and several methods examining the mRNA, protein and functional level to get a complex outlook on the topic.

First, we investigated the cortical glia in the animal model that is used to study ALS the most – the SOD1(G93A) mouse. We confirmed the model´s phenotype using behavioral testing, including identification of differences between males and females. Furthermore, we focused on the changes on the molecular level. The transcriptomic analysis revealed that cortical astrocytes are not affected by the pathology, microglia display features of starting activation and oligodendrocytes seemed to be affected the most as we identified a SOD1-specific oligodendroglial population. The immunohistochemistry then confirmed our assumptions that the overall impact of ALS-like pathology on the cortex is minimal in this model, and it does not reliably mimic the patients´ pathology; however, the presence of the SOD1-specific oligodendrocytes adds to the growing evidence of their active involvement in neurodegeneration.

Even though the astrocytes did not exhibit any ALS-related changes in the cortex of the SOD1(G93A) mouse model, they are an important element in the disease due to their homeostatic functions, which we aimed to investigate further. Results of our experiments using the SOD1(G93A) animal model on FVB/N background revealed astrocytic activation in both the cortex and spinal cord and overall worse gross phenotype of the mice, which was most likely caused by the different genetic background. The functional measurements of swelling showed diminished K^+ uptake of spinal astrocytes during hyperkalemia, which was also confirmed by the RTI method showing an increase in ECS volume fraction. Based on the results from immunohistochemical analysis of Kir4.1 expression, we assume the inefficient

uptake could be associated with a lower expression of this channel as it was downregulated in the spinal cord only.

The analysis of astrocytic functional properties and the ECS in AD revealed an increase in the diffusion barriers that occurred earlier in AD mice compared to the age-matched controls. These changes are most likely associated with the structural shifts caused by the pathology. However, we proved that they do not affect the ECS shrinkage during application of hyperkalemia or hypo-osmotic stress. On the other hand, they seem to affect the astrocytic ability of K^+ uptake as we have observed a diminished swelling during hyperkalemia in 3M and 12M animals.

Altogether, glial cells are an important component in the ALS as they are essential for proper CNS functioning. When affected by the pathology they acquire activated morphology accompanied by alterations in their transcriptional profile as well as protein expression. These lead to changes in glial functions, which can in turn further influence the CNS environment and contribute to neurodegeneration. Our results provided new insights especially into the homeostatic abilities of astrocytes in ALS as well as in AD, but also highlighted the importance of working with reliable disease models in order to further understand the pathology and advance in efforts to find a suitable therapeutic approach.

7 SUMMARY IN ENGLISH

7.1 Characterization of SOD1(G93A) Mouse Model Phenotype and Pathological Trait in the Motor Cortex

We studied the ALS-pathology in the cortex of SOD1(G93A) animals throughout the disease progression and looked for pathological changes in glial cells using scRNA-seq and immunohistochemistry. Our analyses revealed no alterations in astrocytes and only minor changes in microglia and oligodendrocytes at the final stage. The results indicate early stages of activation, but the degree of these changes does not align with those observed in human tissue, supporting the argument against using this model to study ALS pathology in the cortex.

7.2 Functional Properties of Astrocytes in a Mouse Model of Amyotrophic lateral sclerosis

To continue revealing the role of glial cells in ALS, we focused on the astrocytes and their ability to maintain ion homeostasis. We confirmed variability between animal models caused by a different genetic background and observed astrocytic activation in the cortex as well as in the spinal cord. Our functional measurements revealed a spinal cord-specific impairment of astrocytic K^+ uptake during hyperkalemia, manifested also as changes of ECS values. Based on immunohistochemistry, this impairment is likely associated with a reduction of Kir4.1 expression.

7.3 Functional Properties of Astrocytes in a Model of Alzheimer´s Disease

To extend the knowledge about astrocytic functioning during pathology, we examined their swelling/volume regulation ability together with ECS values assessment also in the model of AD. Our results revealed an increase in diffusion barriers in AD mice, which further influenced astrocytic uptake of ions manifested as reduced swelling in response to hypo-osmotic stress or hyperkalemia. Overall,

our data suggest that from the standpoint of astrocytic uptake and water regulation, AD can be understood as an accelerated form of physiological aging.

8 SUMMARY IN CZECH

8.1 Charakterizace fenotypu a patologie v mozkové kůře myšího modelu SOD1(G93A)

V této práci jsme studovali ALS patologii v mozkové kůře SOD1(G93A) myší v průběhu progrese onemocnění a soustředili jsme se na patologické změny gliových buněk s využitím sekvenování na úrovni jedné buňky a imunohistochemie. Naše experimenty neodhalily žádné změny v případě astrocytů a pouze mírné změny u mikroglií a oligodendrocytů ve finálním stádiu onemocnění. Tyto výsledky sice naznačují počínající aktivaci, ale nejsou v souladu se závažností změn, která byla v tomto stádiu pozorována u pacientů, což podporuje spekulace, že by tento model neměl být využíván pro studium ALS patologie v mozkové kůře.

8.2 Funkční vlastnosti astrocytů v myším modelu Amyotrofické laterální sklerózy

V rámci dalšího zkoumání role glií v ALS, jsme se zaměřili na astrocyty a homeostatické vlastnosti při udržování homeostázy iontů. Potvrdili jsme variabilitu mezi myšími modely způsobenou rozdílným genetickým pozadím a pozorovali jsme aktivaci astrocytů jak v mozkové kůře, tak v míše. Naše funkční měření odhalila nedostatečné vychytávání K^+ iontů během hyperkalémie u míšních astrocytů, což se projevilo také změnami v extracelulárním prostoru. K tomuto nedostatečnému vychytávání dochází pravděpodobně v důsledku snížené exprese kanálu Kir4.1, která byla zjištěna pomocí imunohistochemické analýzy.

8.3 Funkční vlastnosti astrocytů v myším modelu Alzheimerovy choroby

Abychom rozšířili znalosti o fungování astrocytů během patologií, zkoumali jsme jejich schopnost regulovat objem společně se změnami extracelulárního prostředí také v modelu AD. Naše výsledky ukázaly zvýšené množství difúzních bariér u myší s AD, což ovlivnilo schopnost astrocytů vychytávat ionty a projevilo se sníženým ‚swellingem' a to jak v prostředí hyperkalémie, tak během hypoosmotického stresu.

Celkově naše data naznačují, že z pohledu objemové regulace astrocytů lze patologické procesy spojené s AD chápat jako zrychlenou formu fyziologického stárnutí.

9 REFERENCES

1. ABRAMOV, A. Y., CANEVARI, L. & DUCHEN, M. R. 2003. Changes in intracellular calcium and glutathione in astrocytes as the primary mechanism of amyloid neurotoxicity. *J Neurosci,* 23**,** 5088-95.
2. ABRAMOV, A. Y., CANEVARI, L. & DUCHEN, M. R. 2004. Beta-amyloid peptides induce mitochondrial dysfunction and oxidative stress in astrocytes and death of neurons through activation of NADPH oxidase. *J Neurosci,* 24**,** 565-75.
3. ALEXIANU, M. E., HO, B. K., MOHAMED, A. H., LA BELLA, V., SMITH, R. G. & APPEL, S. H. 1994. The role of calcium-binding proteins in selective motoneuron vulnerability in amyotrophic lateral sclerosis. *Ann Neurol,* 36**,** 846-58.
4. BAKER, D. J., BLACKBURN, D. J., KEATINGE, M., SOKHI, D., VISKAITIS, P., HEATH, P. R., FERRAIUOLO, L., KIRBY, J. & SHAW, P. J. 2015. Lysosomal and phagocytic activity is increased in astrocytes during disease progression in the SOD1 (G93A) mouse model of amyotrophic lateral sclerosis. *Front Cell Neurosci,* 9**,** 410.
5. BATAVELJIC, D., NIKOLIC, L., MILOSEVIC, M., TODOROVIC, N. & ANDJUS, P. R. 2012. Changes in the astrocytic aquaporin-4 and inwardly rectifying potassium channel expression in the brain of the amyotrophic lateral sclerosis SOD1(G93A) rat model. *Glia,* 60**,** 1991-2003.
6. BEKKU, Y., VARGOVA, L., GOTO, Y., VORISEK, I., DMYTRENKO, L., NARASAKI, M., OHTSUKA, A., FASSLER, R., NINOMIYA, Y., SYKOVA, E. & OOHASHI, T. 2010. Bral1: its role in diffusion barrier formation and conduction velocity in the CNS. *J Neurosci,* 30**,** 3113-23.
7. BEN HAIM, L., CEYZERIAT, K., CARRILLO-DE SAUVAGE, M. A., AUBRY, F., AUREGAN, G., GUILLERMIER, M., RUIZ, M., PETIT, F., HOUITTE, D., FAIVRE, E., VANDESQUILLE, M., ARON-BADIN, R., DHENAIN, M., DEGLON, N., HANTRAYE, P., BROUILLET, E., BONVENTO, G. & ESCARTIN, C. 2015. The JAK/STAT3 pathway is a common inducer of astrocyte reactivity in Alzheimer's and Huntington's diseases. *J Neurosci,* 35**,** 2817-29.
8. BOILLÉE, S., YAMANAKA, K., LOBSIGER, C. S., COPELAND, N. G., JENKINS, N. A., KASSIOTIS, G., KOLLIAS, G. & CLEVELAND, D. W. 2006. Onset and Progression in Inherited ALS Determined by Motor Neurons and Microglia. *Science,* 312**,** 1389-1392.
9. BUTOVSKY, O. & WEINER, H. L. 2018. Microglial signatures and their role in health and disease. *Nat Rev Neurosci,* 19**,** 622-635.
10. DAVALOS, D., GRUTZENDLER, J., YANG, G., KIM, J. V., ZUO, Y., JUNG, S., LITTMAN, D. R., DUSTIN, M. L. & GAN, W. B. 2005. ATP mediates rapid microglial response to local brain injury in vivo. *Nat Neurosci,* 8**,** 752-8.

11. DING, F., SUN, Q., LONG, C., RASMUSSEN, R. N., PENG, S., XU, Q., KANG, N., SONG, W., WEIKOP, P., GOLDMAN, S. A. & NEDERGAARD, M. 2024. Dysregulation of extracellular potassium distinguishes healthy ageing from neurodegeneration. *Brain,* 147**,** 1726-1739.
12. DUYCKAERTS, C., DELATOUR, B. & POTIER, M. C. 2009. Classification and basic pathology of Alzheimer disease. *Acta Neuropathol,* 118**,** 5-36.
13. FALCAO, A. M., VAN BRUGGEN, D., MARQUES, S., MEIJER, M., JAKEL, S., AGIRRE, E., SAMUDYATA, FLORIDDIA, E. M., VANICHKINA, D. P., FFRENCH-CONSTANT, C., WILLIAMS, A., GUERREIRO-CACAIS, A. O. & CASTELO-BRANCO, G. 2018. Disease-specific oligodendrocyte lineage cells arise in multiple sclerosis. *Nat Med,* 24**,** 1837-1844.
14. FLORIDDIA, E. M., LOURENCO, T., ZHANG, S., VAN BRUGGEN, D., HILSCHER, M. M., KUKANJA, P., GONCALVES DOS SANTOS, J. P., ALTINKOK, M., YOKOTA, C., LLORENS-BOBADILLA, E., MULINYAWE, S. B., GRAOS, M., SUN, L. O., FRISEN, J., NILSSON, M. & CASTELO-BRANCO, G. 2020. Distinct oligodendrocyte populations have spatial preference and different responses to spinal cord injury. *Nat Commun,* 11**,** 5860.
15. GERBER, Y. N., SABOURIN, J. C., RABANO, M., VIVANCO, M. & PERRIN, F. E. 2012. Early functional deficit and microglial disturbances in a mouse model of amyotrophic lateral sclerosis. *PLoS One,* 7**,** e36000.
16. GOMES, C., CUNHA, C., NASCIMENTO, F., RIBEIRO, J. A., VAZ, A. R. & BRITES, D. 2019. Cortical Neurotoxic Astrocytes with Early ALS Pathology and miR-146a Deficit Replicate Gliosis Markers of Symptomatic SOD1G93A Mouse Model. *Mol Neurobiol,* 56**,** 2137-2158.
17. GOMES, C., SEQUEIRA, C., BARBOSA, M., CUNHA, C., VAZ, A. R. & BRITES, D. 2020. Astrocyte regional diversity in ALS includes distinct aberrant phenotypes with common and causal pathological processes. *Exp Cell Res,* 395**,** 112209.
18. GURNEY, M. E., PU, H., CHIU, A. Y., DAL CANTO, M. C., POLCHOW, C. Y., ALEXANDER, D. D., CALIENDO, J., HENTATI, A., KWON, Y. W., DENG, H. X. & ET AL. 1994. Motor neuron degeneration in mice that express a human Cu,Zn superoxide dismutase mutation. *Science,* 264**,** 1772-5.
19. HABIB, N., MCCABE, C., MEDINA, S., VARSHAVSKY, M., KITSBERG, D., DVIR-SZTERNFELD, R., GREEN, G., DIONNE, D., NGUYEN, L., MARSHALL, J. L., CHEN, F., ZHANG, F., KAPLAN, T., REGEV, A. & SCHWARTZ, M. 2020. Disease-associated astrocytes in Alzheimer's disease and aging. *Nat Neurosci,* 23**,** 701-706.
20. HALL, E. D., OOSTVEEN, J. A. & GURNEY, M. E. 1998. Relationship of microglial and astrocytic activation to disease onset and progression in a transgenic model of familial ALS. *Glia,* 23**,** 249-56.

21. HEIMAN-PATTERSON, T. D., SHER, R. B., BLANKENHORN, E. A., ALEXANDER, G., DEITCH, J. S., KUNST, C. B., MARAGAKIS, N. & COX, G. 2011. Effect of genetic background on phenotype variability in transgenic mouse models of amyotrophic lateral sclerosis: a window of opportunity in the search for genetic modifiers. *Amyotroph Lateral Scler,* 12**,** 79-86.
22. HOWLAND, D. S., LIU, J., SHE, Y., GOAD, B., MARAGAKIS, N. J., KIM, B., ERICKSON, J., KULIK, J., DEVITO, L., PSALTIS, G., DEGENNARO, L. J., CLEVELAND, D. W. & ROTHSTEIN, J. D. 2002. Focal loss of the glutamate transporter EAAT2 in a transgenic rat model of SOD1 mutant-mediated amyotrophic lateral sclerosis (ALS). *Proceedings of the National Academy of Sciences of the United States of America,* 99**,** 1604-1609.
23. HYND, M. R., SCOTT, H. L. & DODD, P. R. 2004. Glutamate-mediated excitotoxicity and neurodegeneration in Alzheimer's disease. *Neurochem Int,* 45**,** 583-95.
24. JAKEL, S., AGIRRE, E., MENDANHA FALCAO, A., VAN BRUGGEN, D., LEE, K. W., KNUESEL, I., MALHOTRA, D., FFRENCH-CONSTANT, C., WILLIAMS, A. & CASTELO-BRANCO, G. 2019. Altered human oligodendrocyte heterogeneity in multiple sclerosis. *Nature,* 566**,** 543-547.
25. KAISER, M., MALETZKI, I., HULSMANN, S., HOLTMANN, B., SCHULZ-SCHAEFFER, W., KIRCHHOFF, F., BAHR, M. & NEUSCH, C. 2006. Progressive loss of a glial potassium channel (KCNJ10) in the spinal cord of the SOD1 (G93A) transgenic mouse model of amyotrophic lateral sclerosis. *J Neurochem,* 99**,** 900-12.
26. KANG, S. H., LI, Y., FUKAYA, M., LORENZINI, I., CLEVELAND, D. W., OSTROW, L. W., ROTHSTEIN, J. D. & BERGLES, D. E. 2013. Degeneration and impaired regeneration of gray matter oligodendrocytes in amyotrophic lateral sclerosis. *Nat Neurosci,* 16**,** 571-9.
27. KAUR, A., SHUKEN, S., YANG, A. C. & IRAM, T. 2023. A protocol for collection and infusion of cerebrospinal fluid in mice. *STAR Protoc,* 4**,** 102015.
28. KAWAMATA, H., NG, S. K., DIAZ, N., BURSTEIN, S., MOREL, L., OSGOOD, A., SIDER, B., HIGASHIMORI, H., HAYDON, P. G., MANFREDI, G. & YANG, Y. 2014. Abnormal intracellular calcium signaling and SNARE-dependent exocytosis contributes to SOD1G93A astrocyte-mediated toxicity in amyotrophic lateral sclerosis. *J Neurosci,* 34**,** 2331-48.
29. KAYA, T., MATTUGINI, N., LIU, L., JI, H., CANTUTI-CASTELVETRI, L., WU, J., SCHIFFERER, M., GROH, J., MARTINI, R., BESSON-GIRARD, S., KAJI, S., LIESZ, A., GOKCE, O. & SIMONS, M. 2022. CD8(+) T cells induce interferon-responsive oligodendrocytes and microglia in white matter aging. *Nat Neurosci,* 25**,** 1446-1457.

30. KELLEY, K. W., BEN HAIM, L., SCHIRMER, L., TYZACK, G. E., TOLMAN, M., MILLER, J. G., TSAI, H. H., CHANG, S. M., MOLOFSKY, A. V., YANG, Y., PATANI, R., LAKATOS, A., ULLIAN, E. M. & ROWITCH, D. H. 2018. Kir4.1-Dependent Astrocyte-Fast Motor Neuron Interactions Are Required for Peak Strength. *Neuron,* 98**,** 306-319 e7.
31. KENIGSBUCH, M., BOST, P., HALEVI, S., CHANG, Y., CHEN, S., MA, Q., HAJBI, R., SCHWIKOWSKI, B., BODENMILLER, B., FU, H., SCHWARTZ, M. & AMIT, I. 2022. A shared disease-associated oligodendrocyte signature among multiple CNS pathologies. *Nat Neurosci,* 25**,** 876-886.
32. KEREN-SHAUL, H., SPINRAD, A., WEINER, A., MATCOVITCH-NATAN, O., DVIR-SZTERNFELD, R., ULLAND, T. K., DAVID, E., BARUCH, K., LARA-ASTAISO, D., TOTH, B., ITZKOVITZ, S., COLONNA, M., SCHWARTZ, M. & AMIT, I. 2017. A Unique Microglia Type Associated with Restricting Development of Alzheimer's Disease. *Cell,* 169**,** 1276-1290 e17.
33. KOLENICOVA, D., TURECKOVA, J., PUKAJOVA, B., HARANTOVA, L., KRISKA, J., KIRDAJOVA, D., VORISEK, I., KAMENICKA, M., VALIHRACH, L., ANDROVIC, P., KUBISTA, M., VARGOVA, L. & ANDEROVA, M. 2020. High potassium exposure reveals the altered ability of astrocytes to regulate their volume in the aged hippocampus of GFAP/EGFP mice. *Neurobiol Aging,* 86**,** 162-181.
34. KULIJEWICZ-NAWROT, M., VERKHRATSKY, A., CHVATAL, A., SYKOVA, E. & RODRIGUEZ, J. J. 2012. Astrocytic cytoskeletal atrophy in the medial prefrontal cortex of a triple transgenic mouse model of Alzheimer's disease. *J Anat,* 221**,** 252-62.
35. KUO, J. J., SCHONEWILLE, M., SIDDIQUE, T., SCHULTS, A. N., FU, R., BAR, P. R., ANELLI, R., HECKMAN, C. J. & KROESE, A. B. 2004. Hyperexcitability of cultured spinal motoneurons from presymptomatic ALS mice. *J Neurophysiol,* 91**,** 571-5.
36. KUO, J. J., SIDDIQUE, T., FU, R. & HECKMAN, C. J. 2005. Increased persistent Na(+) current and its effect on excitability in motoneurones cultured from mutant SOD1 mice. *J Physiol,* 563**,** 843-54.
37. LEE, S. H., REZZONICO, M. G., FRIEDMAN, B. A., HUNTLEY, M. H., MEILANDT, W. J., PANDEY, S., CHEN, Y. J., EASTON, A., MODRUSAN, Z., HANSEN, D. V., SHENG, M. & BOHLEN, C. J. 2021. TREM2-independent oligodendrocyte, astrocyte, and T cell responses to tau and amyloid pathology in mouse models of Alzheimer disease. *Cell Rep,* 37**,** 110158.
38. LONGINETTI, E. & FANG, F. 2019. Epidemiology of amyotrophic lateral sclerosis: an update of recent literature. *Curr Opin Neurol,* 32**,** 771-776.
39. MANIATIS, S., AIJO, T., VICKOVIC, S., BRAINE, C., KANG, K., MOLLBRINK, A., FAGEGALTIER, D., ANDRUSIVOVA, Z.,

SAARENPAA, S., SAIZ-CASTRO, G., CUEVAS, M., WATTERS, A., LUNDEBERG, J., BONNEAU, R. & PHATNANI, H. 2019. Spatiotemporal dynamics of molecular pathology in amyotrophic lateral sclerosis. *Science,* 364**,** 89-93.

40. MARQUES, S., ZEISEL, A., CODELUPPI, S., VAN BRUGGEN, D., MENDANHA FALCAO, A., XIAO, L., LI, H., HARING, M., HOCHGERNER, H., ROMANOV, R. A., GYLLBORG, D., MUNOZ MANCHADO, A., LA MANNO, G., LONNERBERG, P., FLORIDDIA, E. M., REZAYEE, F., ERNFORS, P., ARENAS, E., HJERLING-LEFFLER, J., HARKANY, T., RICHARDSON, W. D., LINNARSSON, S. & CASTELO-BRANCO, G. 2016. Oligodendrocyte heterogeneity in the mouse juvenile and adult central nervous system. *Science,* 352**,** 1326-1329.
41. MARTINEZ-MURIANA, A., MANCUSO, R., FRANCOS-QUIJORNA, I., OLMOS-ALONSO, A., OSTA, R., PERRY, V. H., NAVARRO, X., GOMEZ-NICOLA, D. & LOPEZ-VALES, R. 2016. CSF1R blockade slows the progression of amyotrophic lateral sclerosis by reducing microgliosis and invasion of macrophages into peripheral nerves. *Sci Rep,* 6**,** 25663.
42. MATHYS, H., ADAIKKAN, C., GAO, F., YOUNG, J. Z., MANET, E., HEMBERG, M., DE JAGER, P. L., RANSOHOFF, R. M., REGEV, A. & TSAI, L. H. 2017. Temporal Tracking of Microglia Activation in Neurodegeneration at Single-Cell Resolution. *Cell Rep,* 21**,** 366-380.
43. MEAD, R. J., SHAN, N., REISER, H. J., MARSHALL, F. & SHAW, P. J. 2023. Amyotrophic lateral sclerosis: a neurodegenerative disorder poised for successful therapeutic translation. *Nat Rev Drug Discov,* 22**,** 185-212.
44. MIGLIARINI, S., SCARICAMAZZA, S., VALLE, C., FERRI, A., PASQUALETTI, M. & FERRARO, E. 2021. Microglia Morphological Changes in the Motor Cortex of hSOD1(G93A) Transgenic ALS Mice. *Brain Sci,* 11.
45. MILLER, S. J., GLATZER, J. C., HSIEH, Y. C. & ROTHSTEIN, J. D. 2018. Cortical astroglia undergo transcriptomic dysregulation in the G93A SOD1 ALS mouse model. *J Neurogenet,* 32**,** 322-335.
46. MINATI, L., EDGINTON, T., BRUZZONE, M. G. & GIACCONE, G. 2009. Current concepts in Alzheimer's disease: a multidisciplinary review. *Am J Alzheimers Dis Other Demen,* 24**,** 95-121.
47. MULLER, M. & SOMJEN, G. G. 2000. Na(+) and K(+) concentrations, extra- and intracellular voltages, and the effect of TTX in hypoxic rat hippocampal slices. *J Neurophysiol,* 83**,** 735-45.
48. NAGAI, M., RE, D. B., NAGATA, T., CHALAZONITIS, A., JESSELL, T. M., WICHTERLE, H. & PRZEDBORSKI, S. 2007. Astrocytes expressing ALS-linked mutated SOD1 release factors selectively toxic to motor neurons. *Nat Neurosci,* 10**,** 615-22.
49. NAGELE, R. G., D'ANDREA, M. R., LEE, H., VENKATARAMAN, V. & WANG, H. Y. 2003. Astrocytes accumulate A beta 42 and give rise to

astrocytic amyloid plaques in Alzheimer disease brains. *Brain Res,* 971**,** 197-209.
50. NAGELE, R. G., WEGIEL, J., VENKATARAMAN, V., IMAKI, H., WANG, K. C. & WEGIEL, J. 2004. Contribution of glial cells to the development of amyloid plaques in Alzheimer's disease. *Neurobiol Aging,* 25**,** 663-74.
51. NIESSEN, H. G., ANGENSTEIN, F., SANDER, K., KUNZ, W. S., TEUCHERT, M., LUDOLPH, A. C., HEINZE, H. J., SCHEICH, H. & VIELHABER, S. 2006. In vivo quantification of spinal and bulbar motor neuron degeneration in the G93A-SOD1 transgenic mouse model of ALS by T2 relaxation time and apparent diffusion coefficient. *Exp Neurol,* 201**,** 293-300.
52. NIKODEMOVA, M. & WATTERS, J. J. 2011. Outbred ICR/CD1 mice display more severe neuroinflammation mediated by microglial TLR4/CD14 activation than inbred C57Bl/6 mice. *Neuroscience,* 190**,** 67-74.
53. NOLTE, C., MATYASH, M., PIVNEVA, T., SCHIPKE, C. G., OHLEMEYER, C., HANISCH, U. K., KIRCHHOFF, F. & KETTENMANN, H. 2001. GFAP promoter-controlled EGFP-expressing transgenic mice: a tool to visualize astrocytes and astrogliosis in living brain tissue. *Glia,* 33**,** 72-86.
54. ODDO, S., CACCAMO, A., SHEPHERD, J. D., MURPHY, M. P., GOLDE, T. E., KAYED, R., METHERATE, R., MATTSON, M. P., AKBARI, Y. & LAFERLA, F. M. 2003. Triple-transgenic model of Alzheimer's disease with plaques and tangles: intracellular Abeta and synaptic dysfunction. *Neuron,* 39**,** 409-21.
55. OLABARRIA, M., NORISTANI, H. N., VERKHRATSKY, A. & RODRIGUEZ, J. J. 2010. Concomitant astroglial atrophy and astrogliosis in a triple transgenic animal model of Alzheimer's disease. *Glia,* 58**,** 831-8.
56. OZDINLER, P. H., BENN, S., YAMAMOTO, T. H., GUZEL, M., BROWN, R. H., JR. & MACKLIS, J. D. 2011. Corticospinal motor neurons and related subcerebral projection neurons undergo early and specific neurodegeneration in hSOD1G(9)(3)A transgenic ALS mice. *J Neurosci,* 31**,** 4166-77.
57. PALMER, A. L. & OUSMAN, S. S. 2018. Astrocytes and Aging. *Front Aging Neurosci,* 10**,** 337.
58. PASANTES-MORALES, H. & VAZQUEZ-JUAREZ, E. 2012. Transporters and channels in cytotoxic astrocyte swelling. *Neurochem Res,* 37**,** 2379-87.
59. PHILIPS, T., BENTO-ABREU, A., NONNEMAN, A., HAECK, W., STAATS, K., GEELEN, V., HERSMUS, N., KUSTERS, B., VAN DEN BOSCH, L., VAN DAMME, P., RICHARDSON, W. D. & ROBBERECHT, W. 2013. Oligodendrocyte dysfunction in the pathogenesis of amyotrophic lateral sclerosis. *Brain,* 136**,** 471-82.
60. PIERI, M., CARUNCHIO, I., CURCIO, L., MERCURI, N. B. & ZONA, C. 2009. Increased persistent sodium current determines cortical

hyperexcitability in a genetic model of amyotrophic lateral sclerosis. *Exp Neurol,* 215**,** 368-79.
61. PIETROBON, D. & MOSKOWITZ, M. A. 2014. Chaos and commotion in the wake of cortical spreading depression and spreading depolarizations. *Nat Rev Neurosci,* 15**,** 379-93.
62. QIAN, K., HUANG, H., PETERSON, A., HU, B., MARAGAKIS, N. J., MING, G. L., CHEN, H. & ZHANG, S. C. 2017. Sporadic ALS Astrocytes Induce Neuronal Degeneration In Vivo. *Stem Cell Reports,* 8**,** 843-855.
63. RANGANATHAN, R., HAQUE, S., COLEY, K., SHEPHEARD, S., COOPER-KNOCK, J. & KIRBY, J. 2020. Multifaceted Genes in Amyotrophic Lateral Sclerosis-Frontotemporal Dementia. *Front Neurosci,* 14**,** 684.
64. RODRIGUEZ, J. J., OLABARRIA, M., CHVATAL, A. & VERKHRATSKY, A. 2009. Astroglia in dementia and Alzheimer's disease. *Cell Death Differ,* 16**,** 378-85.
65. ROITBAK, T. & SYKOVA, E. 1999. Diffusion barriers evoked in the rat cortex by reactive astrogliosis. *Glia,* 28**,** 40-8.
66. ROSSI, D. J., BRADY, J. D. & MOHR, C. 2007. Astrocyte metabolism and signaling during brain ischemia. *Nat Neurosci,* 10**,** 1377-86.
67. SALA FRIGERIO, C., WOLFS, L., FATTORELLI, N., THRUPP, N., VOYTYUK, I., SCHMIDT, I., MANCUSO, R., CHEN, W. T., WOODBURY, M. E., SRIVASTAVA, G., MOLLER, T., HUDRY, E., DAS, S., SAIDO, T., KARRAN, E., HYMAN, B., PERRY, V. H., FIERS, M. & DE STROOPER, B. 2019. The Major Risk Factors for Alzheimer's Disease: Age, Sex, and Genes Modulate the Microglia Response to Abeta Plaques. *Cell Rep,* 27**,** 1293-1306 e6.
68. SCHELTENS, P., DE STROOPER, B., KIVIPELTO, M., HOLSTEGE, H., CHETELAT, G., TEUNISSEN, C. E., CUMMINGS, J. & VAN DER FLIER, W. M. 2021. Alzheimer's disease. *Lancet,* 397**,** 1577-1590.
69. SHINDO, Y., YAMANAKA, R., HOTTA, K. & OKA, K. 2020. Inhibition of Mg(2+) Extrusion Attenuates Glutamate Excitotoxicity in Cultured Rat Hippocampal Neurons. *Nutrients,* 12.
70. STEVENSON, R., SAMOKHINA, E., MANGAT, A., ROSSETTI, I., PURUSHOTHAM, S. S., MALLADI, C. S., MORLEY, J. W. & BUSKILA, Y. 2023. Astrocytic K(+) clearance during disease progression in amyotrophic lateral sclerosis. *Glia,* 71**,** 2456-2472.
71. SYKOVA, E., VORISEK, I., ANTONOVA, T., MAZEL, T., MEYER-LUEHMANN, M., JUCKER, M., HAJEK, M., ORT, M. & BURES, J. 2005. Changes in extracellular space size and geometry in APP23 transgenic mice: a model of Alzheimer's disease. *Proc Natl Acad Sci U S A,* 102**,** 479-84.
72. TAGARELLI, A., PIRO, A., TAGARELLI, G., LAGONIA, P. & QUATTRONE, A. 2006. Alois Alzheimer: a hundred years after the discovery of the eponymous disorder. *Int J Biomed Sci,* 2**,** 196-204.

73. TURECKOVA, J., KAMENICKA, M., KOLENICOVA, D., FILIPI, T., HERMANOVA, Z., KRISKA, J., MESZAROSOVA, L., PUKAJOVA, B., VALIHRACH, L., ANDROVIC, P., ZUCHA, D., CHMELOVA, M., VARGOVA, L. & ANDEROVA, M. 2021. Compromised Astrocyte Swelling/Volume Regulation in the Hippocampus of the Triple Transgenic Mouse Model of Alzheimer's Disease. *Front Aging Neurosci,* 13**,** 783120.
74. VEGH, M. J., HELDRING, C. M., KAMPHUIS, W., HIJAZI, S., TIMMERMAN, A. J., LI, K. W., VAN NIEROP, P., MANSVELDER, H. D., HOL, E. M., SMIT, A. B. & VAN KESTEREN, R. E. 2014. Reducing hippocampal extracellular matrix reverses early memory deficits in a mouse model of Alzheimer's disease. *Acta Neuropathol Commun,* 2**,** 76.
75. YAMANAKA, K., CHUN, S. J., BOILLEE, S., FUJIMORI-TONOU, N., YAMASHITA, H., GUTMANN, D. H., TAKAHASHI, R., MISAWA, H. & CLEVELAND, D. W. 2008. Astrocytes as determinants of disease progression in inherited amyotrophic lateral sclerosis. *Nat Neurosci,* 11**,** 251-3.
76. YASUI, M., OTA, K. & YOSHIDA, M. 1997. Effects of low calcium and magnesium dietary intake on the central nervous system tissues of rats and calcium-magnesium related disorders in the amyotrophic lateral sclerosis focus in the Kii Peninsula of Japan. *Magnes Res,* 10**,** 39-50.
77. YERBURY, J. J., OOI, L., DILLIN, A., SAUNDERS, D. N., HATTERS, D. M., BEART, P. M., CASHMAN, N. R., WILSON, M. R. & ECROYD, H. 2016. Walking the tightrope: proteostasis and neurodegenerative disease. *J Neurochem,* 137**,** 489-505.
78. YOU, J., YOUSSEF, M. M. M., SANTOS, J. R., LEE, J. & PARK, J. 2023. Microglia and Astrocytes in Amyotrophic Lateral Sclerosis: Disease-Associated States, Pathological Roles, and Therapeutic Potential. *Biology (Basel),* 12.
79. ZAMECNIK, J., VARGOVA, L., HOMOLA, A., KODET, R. & SYKOVA, E. 2004. Extracellular matrix glycoproteins and diffusion barriers in human astrocytic tumours. *Neuropathol Appl Neurobiol,* 30**,** 338-50.
80. ZEIS, T., ENZ, L. & SCHAEREN-WIEMERS, N. 2016. The immunomodulatory oligodendrocyte. *Brain Res,* 1641**,** 139-148.

10 LIST OF PUBLICATIONS

Publications related to the thesis:

1. Filipi T, Matusova Z, Abaffy P, Vanatko O, Tureckova J, Benesova S, Kubiskova M, Kirdajova D, Zahumensky J, Valihrach L, Anderova M. Cortical glia in SOD1(G93A) mice are subtly affected by ALS-like pathology. Sci Rep. 2023 Apr 21;13(1):6538. doi: 10.1038/s41598-023-33608-y. PMID: 37085528; PMCID: PMC10121704. IF = 3.8

2. Filipi T, Tureckova J, Vanatko O, Chmelova M, Kubiskova M, Sirotova N, Matejkova S, Vargova L, Anderova M. ALS-like pathology diminishes swelling of spinal astrocytes in the SOD1 animal model. Front Cell Neurosci. In press; IF = 4,2

3. Tureckova J, Kamenicka M, Kolenicova D, Filipi T, Hermanova Z, Kriska J, Meszarosova L, Pukajova B, Valihrach L, Androvic P, Zucha D, Chmelova M, Vargova L, Anderova M. Compromised Astrocyte Swelling/Volume Regulation in the Hippocampus of the Triple Transgenic Mouse Model of Alzheimer's Disease. Front Aging Neurosci. 2022 Jan 27;13:783120. doi: 10.3389/fnagi.2021.783120. PMID: 35153718; PMCID: PMC8829436. IF = 4.504

Other publications:

4. Filipi T, Hermanova Z, Tureckova J, Vanatko O, Anderova AM. Glial Cells-The Strategic Targets in Amyotrophic Lateral Sclerosis Treatment. J Clin Med. 2020 Jan 18;9(1):261. doi: 10.3390/jcm9010261. PMID: 31963681; PMCID: PMC7020059. IF = 4.044